

Optimization of turbine blade cooling with the aim of overall turbine performance enhancement

Authors

Seyyed Morteza Mousavi^{a*}
Amir Nejat^a
Farshad Kowsary^a

^a School of Mechanical Engineering,
College of Engineering, University
of Tehran, Tehran, Iran

ABSTRACT

In the current work, different methods for optimization of turbine blade internal cooling are investigated, to achieve higher cyclic efficiency and output power for a typical gas turbine. A simple two-dimensional model of C3X blade is simulated and validated with available experimental data. The optimization process is performed on this model with two different methods. The first method is a popular method used in previous works with two objectives i.e. the minimization of the maximum temperature and the maximum temperature gradient on the blade. A new method is hereby proposed for optimization of turbine blade cooling, in which the coolant mass flow rate is minimized subject to maximum temperature, and maximum temperature gradient remains lower than certain values. The overall turbine performance is estimated by a simple comparative thermodynamic analysis of the reference design and the representative results obtained from the first and second method of optimization. It is concluded that while the first method of optimization allows higher TIT for a typical turbine, the turbine output power and efficiency could be lower than the reference design, due to high coolant mass flow rate in these candidate points. However, the optimum design point of the second method has higher power output and efficiency compared to all other designs (including reference design) at all values of compressor pressure ratio. It is shown that implementation of the second optimization method can increase the efficiency and the output power of a typical turbine 4.68% and 17% respectively.

Article history:

Received : 8 November 2016
Accepted : 17 January 2017

Keywords: Gas Turbine, CFD, Optimization, Genetic Algorithm, Thermodynamic Analysis.

1. Introduction

The gas turbine performance is highly dependent on turbine inlet temperature (TIT) that is limited by the maximum allowable temperature of material. Several cooling methods are used to protect the turbine blades from the hot gas stream. These cooling methods can be categorized into film cooling and internal cooling methods. Goldstein [1]

described the film cooling as the introduction of a secondary fluid along a surface exposed to a high-temperature environment to protect the surface. Ito et al. [2] studied the effects of film cooling on a gas turbine blade and calculated the film cooling effectiveness downstream of the film holes on surfaces with different curvatures. Han et al. [3] described several internal cooling methods such as jet-impingement cooling, pin-fin cooling, and rib-turbulated cooling, with or without the effects of rotation.

While turbine blade cooling lowers the maximum temperature, it increases the

*Corresponding author: Seyyed Morteza Mousavi
Address: School of Mechanical Engineering, College of Engineering, University of Tehran, Tehran, Iran
E-mail address: mousavi.mor@ut.ac.ir

temperature gradient of a blade, which has a negative effect on durability and lifetime of the material. In addition, the extraction of air from the compressor for cooling purpose reduces the overall efficiency of a gas turbine. Brooks [4] investigated the effects of cooling flow rate on characteristics of a modern gas turbine and demonstrated that each percent of air extraction results in two percent loss in power.

To further increase the power output and efficiency of gas turbines, some researchers optimized shape and location the cooling passages with different objectives. The NASA C3X blade and experimental results of Hylton et al. [5] were most popular for validation of the numerical results. Nowak et al. [6] presented a two-dimensional model of C3X blade and optimized the location and diameter of cooling holes, in order to minimize a linear combination of maximum temperature and temperature variance of the blade. Later, Nowak and Wroblewski [7], [8] presented another optimization method for C3X blade, in which the objective function was a linear combination of maximum temperature and maximum thermal stress of the blade. Other similar studies are by Nowak et al. on internal cooling optimization in [9], [10]. Mazaheri et al. [11] and Nowak et al. [12] conducted a multi-objective optimization to reduce the maximum temperature and maximum temperature gradient simultaneously. Wang et al. [13] compared three different hole configurations to minimize the average temperature of a blade, subject to the condition of thermal stress being lower than the maximum allowable stress of the material.

Most researchers optimized the cooling configuration of a blade with an objective of minimization of temperature or temperature gradient at constant pressure, however, the variation of coolant mass flow rate, which has a direct impact on gas turbine performance, is missed in the mentioned studies. In this research, a new method is presented for optimization, wherein the objective is to reduce the coolant mass flow rate, subject to maximum temperature and maximum temperature gradient values being less or equal to that of the base design. The location and diameter of cooling holes are optimized with both the presented method and the multi-objective method described in [11], [12]. Finally, a simple thermodynamic model is used to compare the estimated turbine cyclic efficiency and output power for the results of both optimization methods.

Nomenclature

y^+	non-dimensional wall distance
\dot{m}	mass flow rate (kg/s)
Re	Reynolds number
Nu	Nusselt number
Pr	Prandtl number
d, D	cooling hole diameter
c	axial chord of the blade
k_{st}	the thermal conductivity of steel
k_{air}	the thermal conductivity of air
	convective heat transfer coefficient
h	air enthalpy (only in the thermodynamic analysis)
T	temperature
P	pressure
S	entropy
$ \nabla T $	the length of the temperature gradient vector
P_r	the pressure ratio of the compressor
x	the ratio of the coolant to compressor mass flow rates
\dot{w}	specific work
\dot{q}	specific heat transfer rate
η	gas turbine overall efficiency

Abbreviations

CFD	Computational Fluid Dynamics
CHT	Conjugate Heat Transfer
TIT	Turbine Inlet Temperature
RANS	Reynolds-averaged Navier-Stokes
GA	Genetic Algorithm
NASA	National Aeronautics and Space Administration

2.Numerical model

2.1.The Geometry

The two-dimensional conjugate heat transfer (CHT) around NASA C3X blade is modelled only once to validate and calculate the heat transfer coefficient distribution around the blade. The solution domain for CHT simulation is depicted in Fig.1. The heat transfer and flow characteristics of cooling holes are estimated by empirical correlations for internal flow. Thus, the holes are not

included in this domain. After simulation of the flow around the blade and extraction of heat transfer coefficient along the blade external surface, only the heat transfer problem in the solid domain should be solved for different hole configurations in the optimization process. The solid domain and the geometrical parameters of the blade and cooling holes are shown in Fig.2.

The C3X blade material is ASTM 310 stainless steel with variable thermal conductivity which can be described in terms of temperature as $K_{St} = 0.01157T + 9.9105 W.(m.K)^{-1}$. Sutherland formulation is used to estimate the viscosity and thermal conductivity of air in different temperatures.

2.2.Governing equations

The flow around the blade is assumed to be compressible and steady state where as turbulence and the effects of gravity and domain. In the case of turbulent flow,

momentum equations are replaced by Reynolds-averaged Navier-Stokes (RANS) equations. The continuity and the RANS equations for fluid domain can be expressed in tensor form as radiation is neglected. The energy equation along with continuity and momentum equations should be solved for the fluid

$$\text{Continuity equation: } \frac{\partial}{\partial x_i}(\rho u_i) = 0 \quad (1)$$

$$\begin{aligned} \text{Momentum equation: } & \frac{\partial u}{\partial x_i}(\rho u_i u_j) = -\frac{\partial p}{\partial x_j} \\ & + \frac{\partial}{\partial x_i} \left[\mu \left(\frac{\partial u_i}{\partial x_j} + \frac{\partial u_j}{\partial x_i} - \frac{2}{3} \sigma_{ij} \frac{\partial u_k}{\partial x_k} \right) \right] \\ & + \frac{\partial}{\partial x_i} (-\rho \overline{u'_i u'_j}) \end{aligned} \quad (2)$$

where the term $\overline{u'_i u'_j}$ in Eq.(2) should be estimated by a proper turbulence model. The energy equation should be solved for both the fluid and solid domains and it can be expressed as

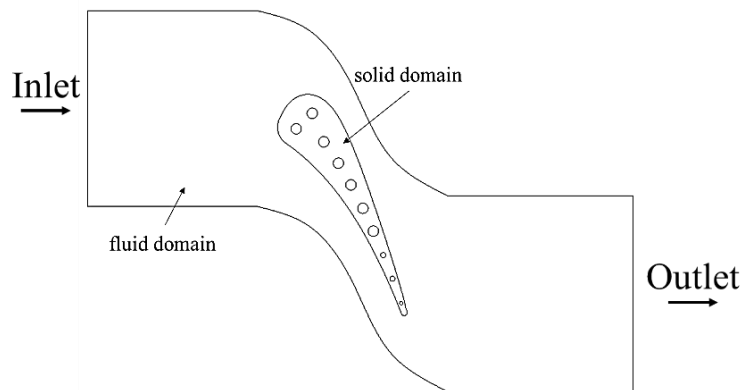


Fig.1. Solution domain used for CHT simulation

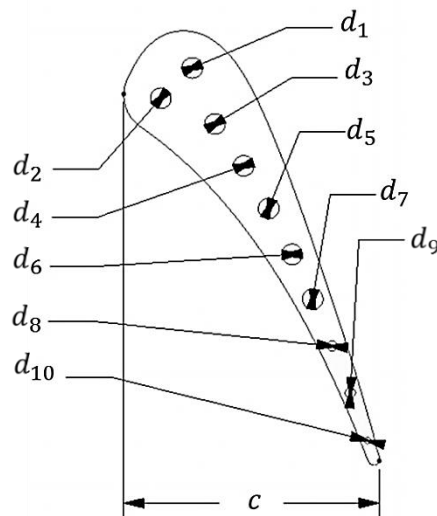


Fig.2. Geometrical parameters of the C3X blade

$$\text{Energy equation: } \frac{\partial}{\partial x_j} (\rho u_j T) = \frac{\partial}{\partial x_j} \left[\left(\frac{\mu}{Pr} + \frac{\mu_t}{\sigma_T} \right) \frac{\partial T}{\partial x_j} \right] \quad (3)$$

where the left-hand side of this equation is equal to zero for the solid domain.

2.3. Boundary conditions

The inlet and outlet boundary conditions are specified according to ‘run 157’ experiments of Hylton et al. [5]. The coupled boundary condition is used for fluid-solid interface and the convective heat transfer of each hole is estimated by its corresponding temperature and heat transfer coefficient. The details of boundary conditions for simulation are presented in Table 1.

The heat transfer coefficient of each hole can be calculated from the experimental correlation of forced convection and Nusselt number of a tube [14].

$$Nu = \frac{hD}{k_{air}} = 0.023Re^{0.8}Pr^{0.4} \quad (4)$$

where Re and Pr stand for Reynolds and Prandtl numbers of fluid, respectively. The mass flow rate and the average temperature of each hole from run 157 are presented in Table 2.

The reference values for mass flow rate and heat transfer coefficient for each hole of the base configuration of C3X blade are known. However, by changing the diameter of holes in optimization process, the \dot{m} and h values should be recalculated according to the hole diameter. By assuming a constant pressure drop for each hole and Darcy-Weisbach equation for pressure loss [15], the mass flow rate and heat transfer coefficient of each hole can be estimated by

$$\dot{m} = \dot{m}_r \left(\frac{D}{D_r} \right)^{2.5} \quad (5)$$

Table 1. Boundary conditions for conjugate heat transfer analysis

Location	B.C. type	Parameter value
Main inlet	Pressure inlet	$P_{tot,m,i} = 413,286Pa$ $T_{m,i} = 818K$ $intensity = 8.3\%$
Outlet	Pressure outlet	$P_{sta,o} = 254,172$
Blade external walls	Coupled wall	$u = v = w = 0$ $k_{st} \frac{\partial T}{\partial \hat{n}} = h(T - T_\infty)$
Internal walls	Wall with Convective heat transfer	$u = v = w = 0$ $k_{st} \frac{\partial T}{\partial \hat{n}} = h_j(T - T_j)$ $j = \text{Hole number}$
Periodic surfaces	Translational periodic	-

Table 2. Dimension, mass flow rate and temperature of each coolant hole

j	D (mm)	\dot{m} (g/s)	T(K)
1	6.3	0.0222	352.14
2	6.3	0.0221	354.54
3	6.3	0.0218	345.62
4	6.3	0.0228	346.72
5	6.3	0.0225	340.7
6	6.3	0.0225	366.21
7	6.3	0.0216	351.48
8	3.1	0.00744	376.24
9	3.1	0.00477	406.97
10	1.98	0.00256	446.69

$$h = h_r \left(\frac{D}{D_r} \right)^{0.2} \tag{6}$$

equations, where \dot{m}_r and h_r are the reference values of mass flow rate and heat transfer coefficient, respectively.

2.4.Optimization

The main objective of this research is to compare different optimization methods for gas turbine blade cooling. The first method is a multi-objective optimization suggested by [11] and [12], in which the objective was to minimize the maximum temperature and the maximum temperature gradient in the blade. The objective functions of the first method can be expressed as

$$minimize : \begin{cases} \max(T) \\ \max(|\nabla T|) \end{cases} \tag{7}$$

where no constraints existed and the coolant mass flow rate might increase during the process. In this study, we offer another optimization method which appears to be more compatible with gas turbines cycle. In this method, the objective is to minimize the coolant mass flow rate, subject to maximum temperature and maximum temperature gradient remaining lower than specific values. The objective function and the constraints of the proposed (second) method can be expressed as:

$$\begin{aligned} &Minimize : \dot{m}_c \tag{8} \\ &Subject To : \begin{cases} \max(|\nabla T|) \leq A \\ \max(T) \leq B \end{cases} \end{aligned}$$

where the values of A and B are selected by their respective values in the reference design.

2.5.Design variables

In the current work, location and diameter of the cooling holes are chosen as the design variables. To reduce the number of the design variables and to keep the holes inside the blade area, the location of the first two holes are kept constant and the other holes are restricted to move only along a certain curve. This curve is a second order polynomial which best fits the initial location of holes as displayed in Fig.3. By using this curve, the location of each of eight holes can be specified by one variable, and in addition to 10 variables for each hole diameter, there will be 18 design variables in total.

2.6.Thermodynamic modelling

A simple turbine with ideal Brayton cycle is assumed for estimation of the effects of the coolant mass flow rate and the turbine inlet temperature on turbine performance. Fig.4 presents the T-S diagram for this cycle between arbitrary P_1 and P_2 pressures. The coolant air is extracted from the compressor

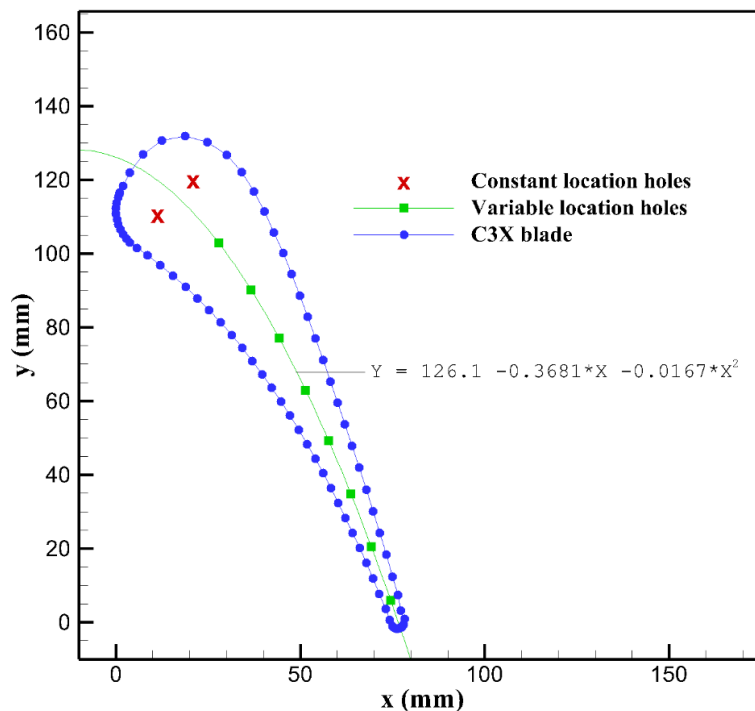


Fig.3. The curve of possible locations for cooling holes

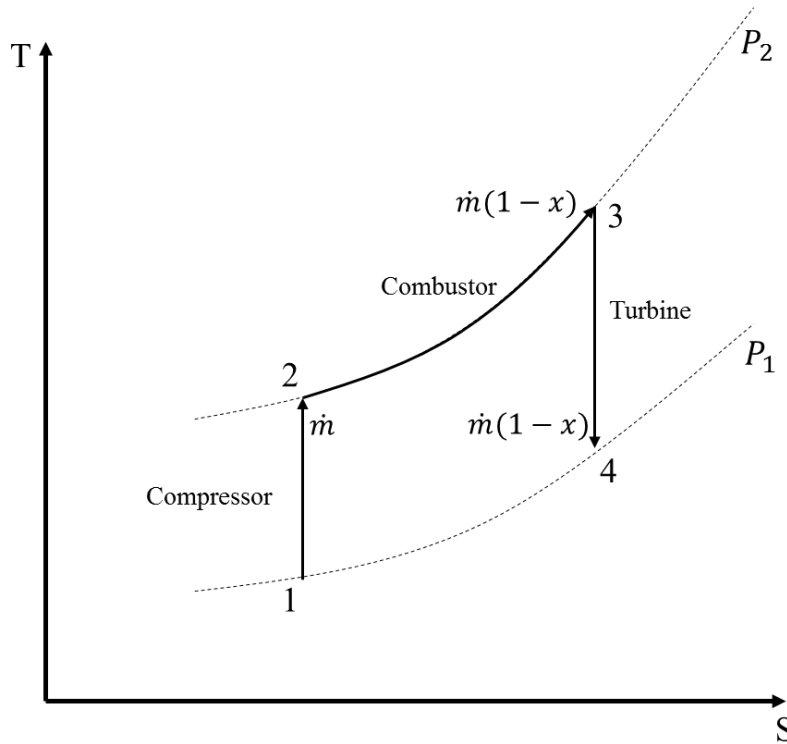


Fig.4. The ideal Brayton cycle with coolant air extracted from compressor outlet

outlet, so the mass flow rate at the combustor and the turbine can be calculated by

$$\dot{m}_{turb} = \dot{m}_{comb} = \dot{m}(1-x) \quad (9)$$

where \dot{m} is the mass flow rate of the compressor and x is the mass flow rate ratio of the coolant to the compressor.

In this cycle, the compressor intake conditions are assumed to be $P_1 = 1 \text{ atm}$ and $T_1 = 300 \text{ K}$. The compressor outlet pressure P_2 , is related to compressor pressure ratio, P_r . By considering a specific value for TIT (T_3), air properties at all points of the cycle can be determined. The turbine specific output power and net output power can be calculated from

$$\dot{w}_{turb} = (1-x)(h_3 - h_4) \quad (10)$$

$$\begin{aligned} \dot{w}_{net} &= \dot{w}_{turb} - \dot{w}_{comp} \\ &= (1-x)(h_3 - h_4) \\ &\quad - (h_2 - h_1) \end{aligned} \quad (11)$$

and the turbine efficiency can be expressed by

$$\begin{aligned} \eta &= \frac{\dot{w}_{net}}{\dot{q}_{comb}} \\ &= \frac{(1-x)(h_3 - h_4) - (h_2 - h_1)}{(1-x)(h_3 - h_2)} \end{aligned} \quad (12)$$

where the real air properties for all points are calculated by the EES software for different cases.

3. Meshing and validation

3.1. Mesh procedure

Unstructured mesh with boundary layer mesh near walls is generated in all cases in this research. Five different meshes with 5.8 up to 24.6 thousand elements are generated for grid independence analysis and the blade temperatures are compared in Fig.5. The results are almost the same for 11.5k and more elements, so this mesh configuration is used for all cases in this research. The selected mesh, which has the y^+ smaller than one near blade walls, is shown in Fig.6.

3.2. Validation

Four different turbulence models are used to perform CHT analysis and the temperature distribution on the blade surface is calculated by each model. The results are compared with experimental data from Hylton et al. [5] in Fig.7. The data on the negative side of the horizontal axis represent the data on the suction side of the blade, and the others represent the pressure side data. It is observed that the SST $\kappa - \omega$ model has the highest accuracy with maximum error of 6% near leading edge of the blade. The heat transfer coefficient on the external blade walls are

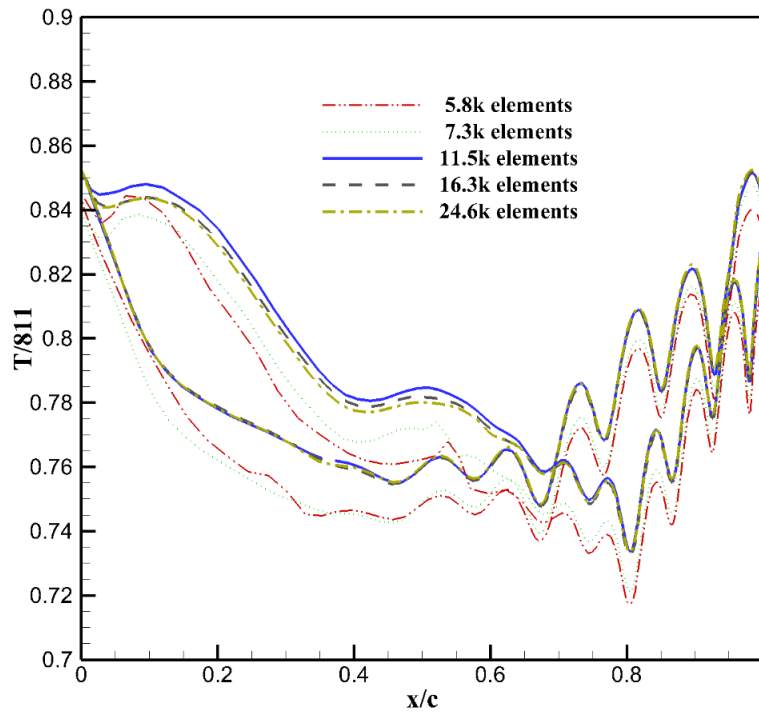


Fig.5. Grid independence analysis

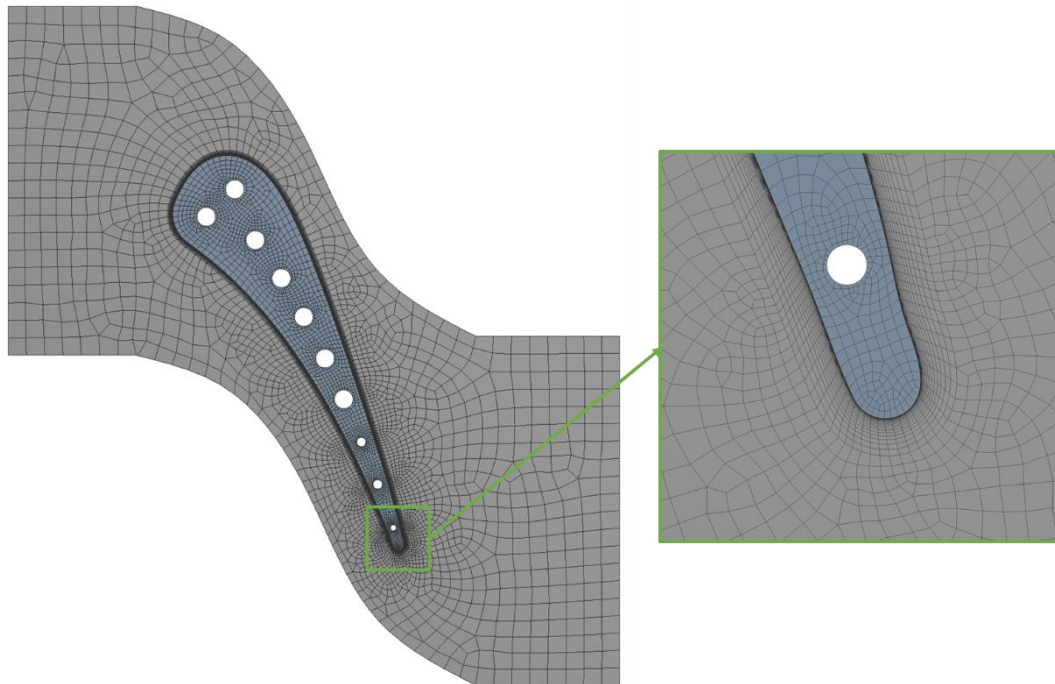


Fig.6. The computing mesh of fluid and solid domains with boundary layer elements

extracted with this model and used as a boundary condition for solid domain in optimization process.

4.Results and discussion

4.1.Reference design

The coolant flow rate, blade maximum temperature and blade maximum gradient are

variables of interest in this section. The values for these variables in reference design are presented in Table 3. According to this table, the A and B values in Eq. (8) are set to be 25000K/m and 685K respectively.

The contours of the blade temperature and temperature gradient in reference design are depicted in Fig.8 (a) and (b), respectively. While the blade leading edge is the most critical point for cooling in most blades, in

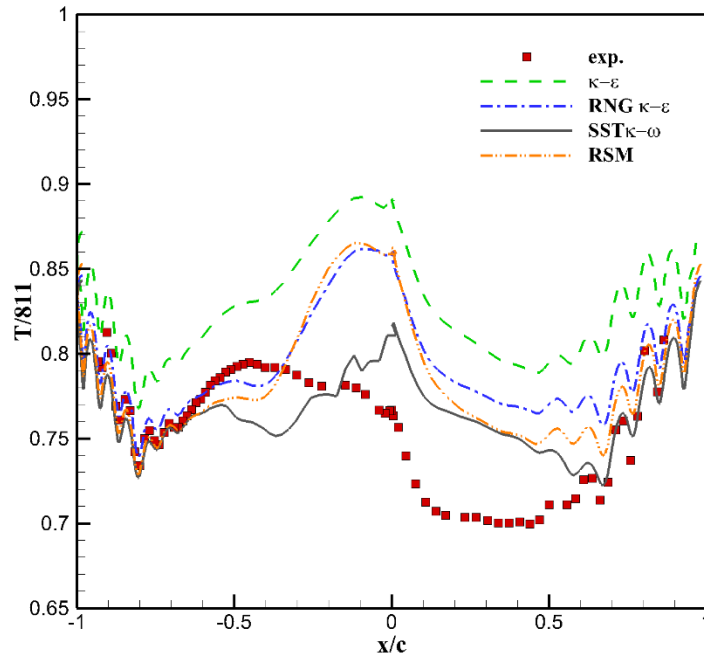
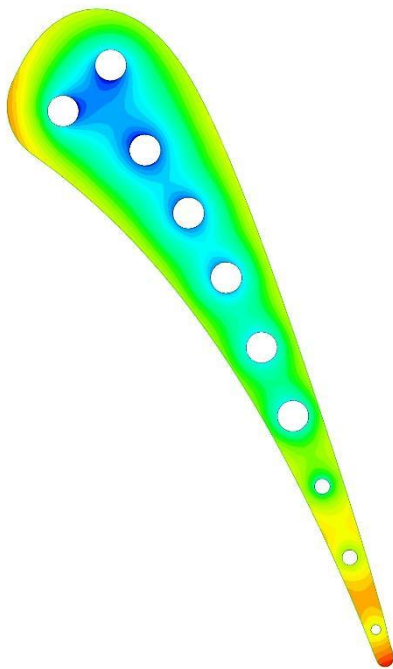
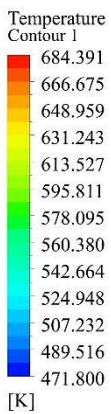


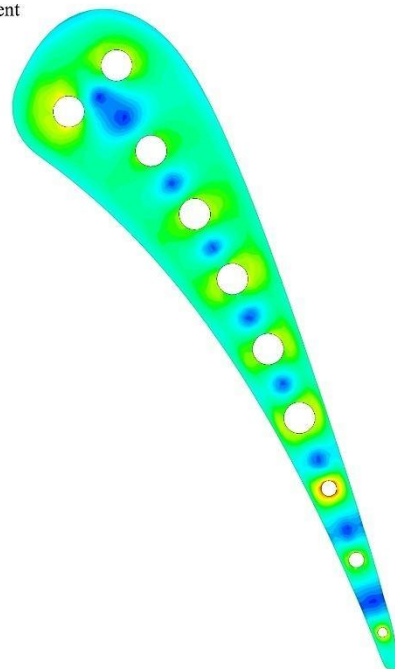
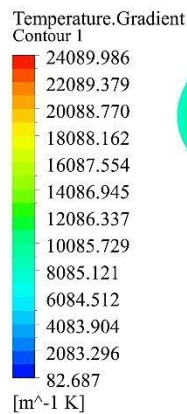
Fig.7. Validation of the results of different turbulence models with experimental data

Table 3. Parameter values in reference design

Parameter	Value	Unit
\dot{m}_c	0.17027	kg/s
$\max(T)$	682.924	K
$\max(\nabla T)$	24090	K/m



(a)



(b)

Fig.8. Contours of field variables in reference design. (a) temperature and (b) temperature gradient

this case, the maximum temperature is observed at the trailing edge area. This is due to high temperature of the coolant flowing through the hole number 10. The temperature gradient is higher near cooling holes, and the highest point is reached near the eighth hole.

4.2. First method of optimization

A multi-objective genetic algorithm is implemented in this method, with the objectives of minimizing the maximum temperature and the maximum temperature gradient of the blade. There is no constraint on coolant mass flow rate, so the value changes freely during the optimization process. An initial population of 400 and 80 populations for the next generations are used for optimization and the solution is converged after 1655 observations. The objective functions of all observations are plotted in Fig.9 and the Pareto front is also displayed.

Four different points on the Pareto front are selected as candidates for best design point and represented by A to D on the chart.

The values for output functions of the candidate points are presented in Table 4. All candidates have a dimensionless coolant mass flow rate of greater than one, and they have different thermal characteristics at the TIT equal to 818K. To find out the maximum allowable TIT in each candidate design point, the TIT for each candidate is increased, until one of the $\max(T)$ or $\max(|\nabla T|)$ becomes higher than 685K or 25,000K/m, respectively. As shown in Table 4, in design point A the maximum temperature gradient is already higher than its value in reference design, thus the TIT cannot be increased in this case. This point is removed from the candidate points for later sections of this research, and the turbine performances for the other three candidates are compared for the rest of the candidates.

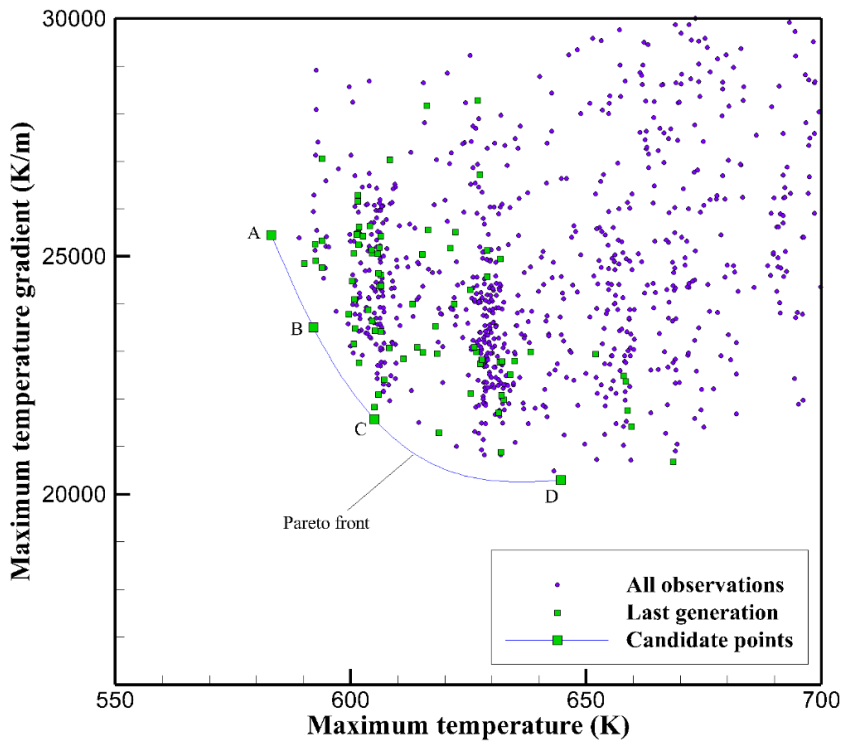


Fig.9. Objective function space for first method optimization

Table 4. The results of first method optimization for each candidate point

Candidate point	TIT = 818 K			Max allowable TIT (K)
	Dimensionless \dot{m}_c	$\max(T)$ (K)	$\max(\nabla T)$ (K/m)	
A	1.789	583.102	25453.800	<818K
B	2.104	592.065	23511.700	843.238
C	1.869	605.067	21573.500	874.952
D	1.237	644.563	20291.800	859.581

The temperature distribution for the design points B, C and D with the TIT equal to 818K are depicted in Fig.10. The design point B has the lowest coolant mass flow rate, so its higher temperature is anticipated.

4.3. Second method of optimization

In this method, the optimization is performed with the objective to minimize the coolant mass flow rate in the same blade, with constraints on maximum temperature and

maximum temperature gradient. The genetic algorithm with 400 initial population and 80 population per next generation, is used to find the optimum design point and the solution converged after almost 1200 observations. The first 400 points are generated randomly and many of them do not satisfy the problem constraints. The objective function values are sorted in ascending order for each generation and the convergence history of the objective function is displayed in Fig.11.

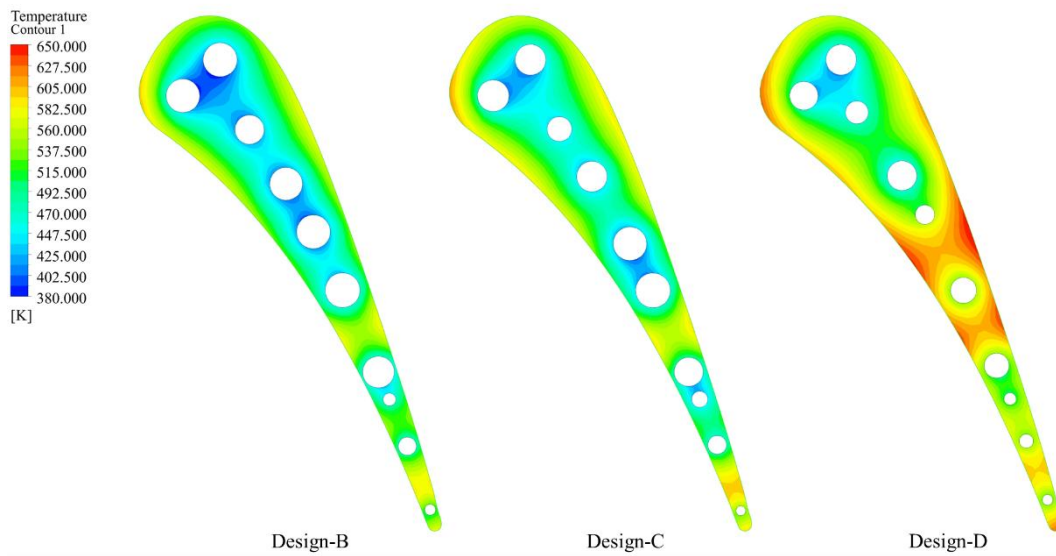


Fig.10. Temperature contours for the three final candidate points

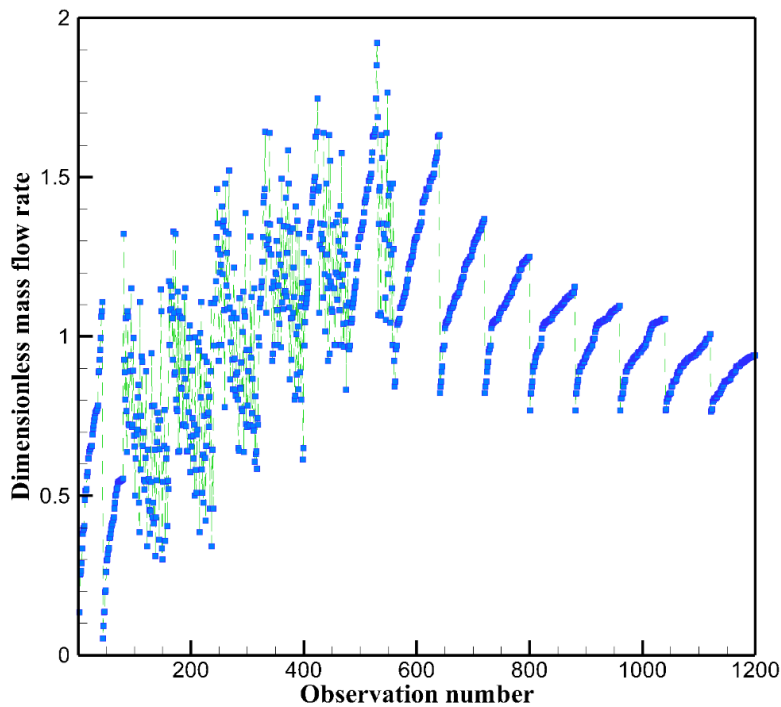


Fig.11. Convergence history of dimensionless mass flow rate

The best design point with minimum objective function and acceptable constraint values has a dimensionless mass flow rate of 0.71, which means 29% reduction in coolant mass flow rate. The values of the design variables and output functions are presented in Table 5.

The contours of the blade temperature and temperature gradient are illustrated in Fig.12 (a) and (b), respectively. The maximum temperature gradient occurs around the holes similar to other cases but the temperature distribution is more uniform compared to the reference design. The very small diameter of the eighth hole means that the number of the holes is more than required for this blade.

4.4. Thermodynamic analysis

The comparison of the turbine performance at different pressure ratios for the three candidate points in the first method, the result of the second method and the reference design have been shown in Fig.13. In the reference design, around 10% of the total mass flow rate is extracted for cooling purpose. Hence, the TIT and x values for the reference design are assumed to be 818K and 0.1, respectively. The results of the first optimization method have higher values of TIT and x , but in second method the x is minimized with the constant TIT. The B and C design points in the first method have lower efficiency and

Table 5. The optimization results of the second method

Variable	Value (mm)	Variable	Value (mm)	Variable	Value (mm)	Output	Value
d_1	6.570	d_7	5.823	x_5	46.456	Dimension less	0.710
d_2	5.312	d_8	0.685	x_6	51.860	\dot{m}_c	682.739 K
d_3	3.545	d_9	3.521	x_7	61.003	$\max(T)$	22435.100 K/m
d_4	6.011	d_{10}	2.444	x_8	63.421	$\max(\nabla T)$	
d_5	4.230	x_3	25.467	x_9	69.567		
d_6	5.922	x_4	35.697	x_{10}	73.816		

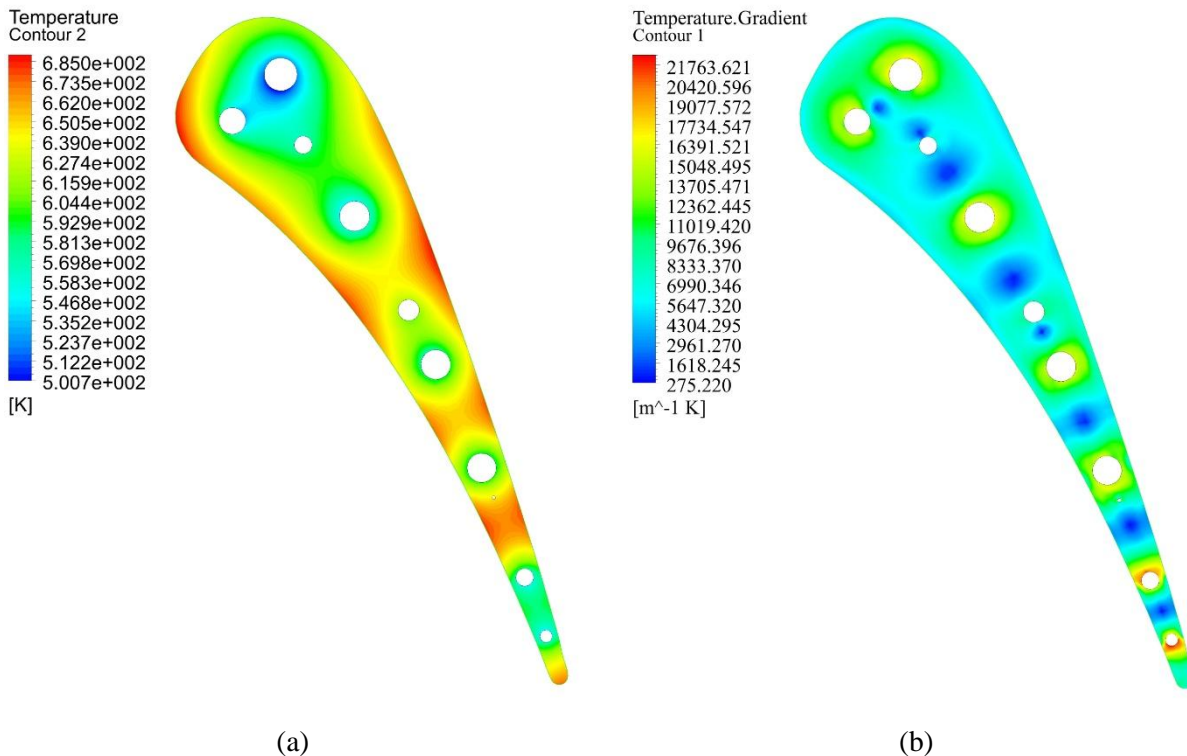


Fig.12. Results of second method optimization. (a) Temperature and (b) temperature gradient contours

power output compared to reference design. In the design point D, the turbine power output is increased but the efficiency has slightly decreased compared to the reference design. But, the optimized geometry in the second method has the higher turbine efficiency and power output with respect to the reference design. So, the second optimization method is more convenient in the case of gas turbine blade cooling optimization.

A typical gas turbine can perform at a pressure ratio of 12 or more. The turbine performance of different designs at this pressure ratio is compared in Table 6. The optimum design of the second optimization method increased the power output of the turbine by 17% compared to reference design and also shows 4.68% higher efficiency. This value will be even higher for a real gas turbine with 15% coolant mass flow rate, where reduction of 1% from coolant mass flow rate can increase the power output by 2% [4].

5. Conclusion

Different methods for optimization of turbine

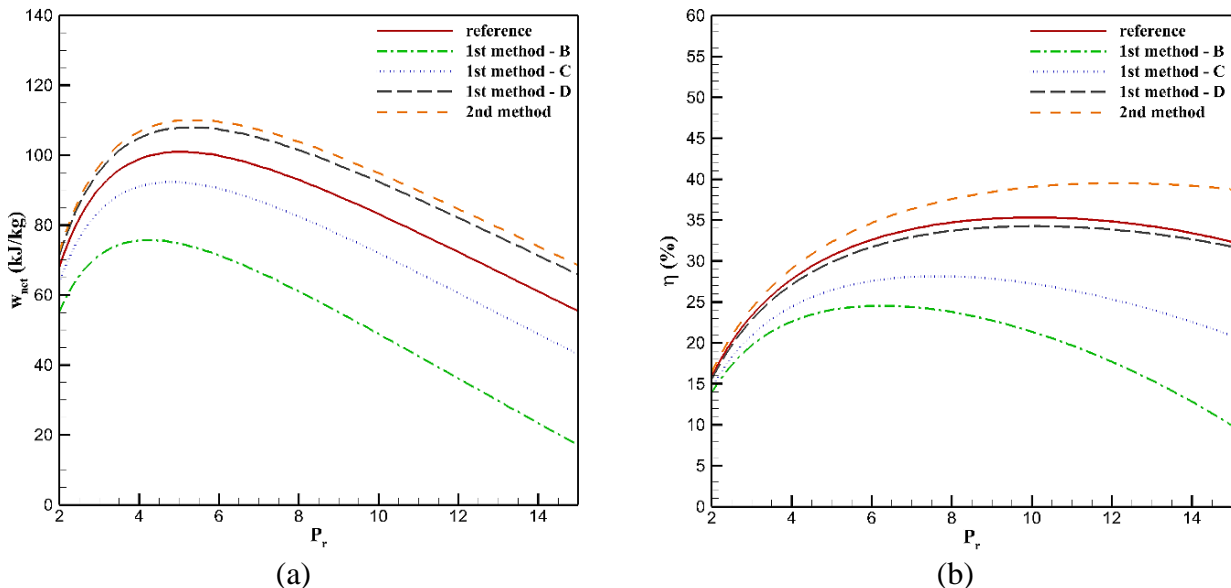


Fig.13. Turbine performance of different designs. (a) net power output and (b) turbine efficiency

Table 6. Gas turbine performance of different designs at $P_r = 12$

Case	TIT (K)	x	\dot{w}_{net} ($\frac{kJ}{kg}$)	η
reference design	818	0.1	72.3	34.83
1st method-B	843.238	0.2104	36.1	17.69
1st method-C	874.952	0.1869	60.5	25.34
1st method-D	859.581	0.1237	82.1	33.84
2nd method	818	0.071	84.6	39.51

blade cooling are discussed and a new optimization method is offered for turbine blade cooling with the aim of improving the overall turbine efficiency and output power. The location and diameter of cooling passages in a 2D model of C3X blade are optimized with two different methods. The first method, which was a popular one in previous research, is a multi-objective method to minimize maximum temperature and maximum temperature gradient in the blade. The second method is proposed in this paper and its objective is to minimize the coolant flow rate required to keep the temperature and temperature gradient lower than a specific value. The performance of the optimum designs of these two methods has been compared by a simple thermodynamic analysis.

The proposed method in this research (second method) is superior to the first method in terms of time consumption and certainty. It is mainly because a multi-objective optimization method requires more time to converge and the user must choose between a series of design points at the Pareto front himself.

The second method's optimum design has

increased the turbine power output and efficiency by 17% and 4.68%, respectively.

However, while the candidate points of first method allow higher TIT without any harm to blades, the turbine performance might deteriorate due to high coolant mass flow rate.

References

- [1] Goldstein R. J., Film Cooling, in *Advances in Heat Transfer* (1971) 321–379.
- [2] Ito S., Goldstein R. J., Eckert E. R. G., Film Cooling of a Gas Turbine Blade, *Journal of Engineering for Power* (1978) 100(3): 476.
- [3] Han J.-C., Dutta S., Ekkad S., *Gas Turbine Heat Transfer and Cooling Technology*, Second Edition (2012) 27.
- [4] Brooks F. J., *GE Gas Turbine Performance Characteristics* (2000).
- [5] Hylton L. D., Mihelc M. S., Turner E. R., Nealy D. A., York R. E., Analytical and Experimental Evaluation of the Heat Transfer Distribution Over the Surfaces of Turbine Vanes (1983).
- [6] Nowak G., Odzimierz Wróblewski W., Chmielniak T., Optimization of Cooling Passages Within a Turbine Vane, *ASME Conference Proceedings* (2005) 47268:519–525.
- [7] Nowak G., Wróblewski W., Thermo Mechanical Optimization of Cooled Turbine Vane, in *Volume 4: Turbo Expo 2007, Parts A and B* (2007) 0: 931–938.
- [8] Nowak G., Wróblewski W., Cooling System Optimisation of Turbine Guide Vane, *Applied Thermal Engineering* (2009) 29(2–3): 567–572.
- [9] Nowak G., Wróblewski W., Nowak I., Convective Cooling Optimization of a Blade for a Supercritical Steam Turbine, *International Journal of Heat and Mass Transfer* (2012) 55(17–18): 4511–4520.
- [10] Nowak G., Nowak I., Shape Design of Internal Cooling Passages within a Turbine Blade, *Optimization and Engineering* (2012) 44(4): 449–466.
- [11] Mazaheri K., Zeinalpour M., Bokaei H. R., Turbine Blade Cooling Passages Optimization Using Reduced Conjugate Heat Transfer Methodology, *Applied Thermal Engineering* (2016) 103:1228–1236.
- [12] Nowak G., Wróblewski W., Optimization of Blade Cooling System with Use of Conjugate Heat Transfer Approach,” *The International Journal of Thermal Sciences* (2011) 50(9):1770–1781.
- [13] Wang B., Zhang W., Xie G., Xu Y., Xiao M., Multiconfiguration Shape Optimization of Internal Cooling Systems of a Turbine Guide Vane Based on Thermomechanical and Conjugate Heat Transfer Analysis, *Journal of Heat Transfer* (2015) 137(6): 61004.
- [14] Bergman T. L., Incropera F. P., DeWitt D. P., Lavine A. S., *Fundamentals of Heat and Mass Transfer*, John Wiley & Sons (2011).
- [15] Fox R. W., McDonald A. T., Pritchard P. J., McDonald A. T., Pritchard P. J., *Introduction to Fluid Mechanics*, John Wiley & Sons New York (1985) 7(1).